Monte Carlo calculation of inter-valence-band radiation absorption in germanium. I. General principles and low-intensity absorption

1989 J. Phys.: Condens. Matter 1 9637

(http://iopscience.iop.org/0953-8984/1/48/013)

J. Phys.: Condens. Matter **1** (1989) 9637–9651. Printed in the UK

Monte Carlo calculation of inter-valence-band radiation absorption in germanium: I. General principles and low-intensity absorption

A Dargys
Institute of Semiconductor Physics, Academy of Sciences of the Lithuanian SSR, 232600 Vilnius, Lithuania, USSR

Received 30 November 1988

Abstract. This is the first of two papers that present general principles of Monte Carlo (MC) simulation of linear and non-linear infrared-radiation absorption due to hole inter-valence transitions in p-type semiconductors. In the MC model the heavy- and light-mass sub-bands are treated as a collection of two-level systems, wherein the hole due to excitations by lattice vibrations hops between different members of the system. The close analogy with the two-level system allows one to incorporate into the MC program such purely quantum-mechanical effects as Rabi oscillations and dephasing. In this paper the general principles are presented and used to calculate absorption cross section at weak laser intensities. High-intensity absorption will be treated in the second paper.

1. Introduction

The Monte Carlo (MC) method as applied to charge carrier transport in semiconductors (Jacoboni and Reggiani 1983) consists of numerical simulation of particle motion and scattering by lattice imperfections in constant or time-varying fields. One of the assumptions implicit in the MC method is that between collisions the particle free flight proceeds in a single energy valley or valence sub-band. The transitions to other sub-bands (valleys) are included through collisions with the phonons, impurity atoms, etc. In strong electric fields, however, the hole or electron, before experiencing the next collision, may appear in another sub-band by a tunnelling effect. The tunnelling probability is large when the energy sub-bands are close enough, such as for example in covalent p-type semiconductors in the vicinity of the degeneracy point, where heavy- (h) and light- (l) mass sub-bands meet. In a laser field the inter-valence tunnelling† of the hole is intense if the energy separation between sub-bands satisfies the resonance conditions.

Our main interest lies in simulating hole dynamics in high-intensity laser fields, when valence-band wavefunction mixing by the laser electric field causes oscillations of

† The terms 'inter-valence tunnelling' and 'inter-valence transition' can be used interchangeably, although the former implies that in finding the transition probability the electric field, constant or alternating, has been considered to be responsible for inter-band transitions (Aleshkin and Romanov 1984, Dargys 1987). We assume that the forbidden energy gap is wide enough so that Zener (1934) tunnelling between valence and conduction bands is absent, and only tunnelling within conduction or valence sub-bands occurs. Electron tunnelling between conduction bands was invoked to explain the dependence of impact ionisation rate upon electric field orientation (Pearsall *et al* 1977). Modulation of the hole velocity between collisions in a constant electric field due to hole tunnelling between valence sub-bands was considered by Dargys (1989a).

0953-8984/89/489637 + 15 $02.50

population of h and l sub-bands in the resonance region (Dargys 1987). Oscillations of energy level population in the laser field are well known in atomic physics, where they are usually referred to as Rabi oscillations (Allen and Eberly 1975). If Rabi oscillations of various atoms in the ensemble have different frequencies or initial phases, then, in addition, dephasing effects will come into play. Rabi oscillations of the hole population in the resonance region and large hole scattering rate in the l sub-band lead to hole burning in the hole distribution function and concurrent bleaching of p-type semiconductors, first observed experimentally by Gibson (1972). References on this subject can be found in a review article by James and Smith (1982).

The standard MC method (Jacoboni and Reggiani 1983) is a classical statistical method, because the complicated particle trajectory in momentum or real space is the result of the simulation of classical particle motion. In this paper the standard classical MC procedure is modified to include quantum-mechanical effects, namely Rabi oscillations and dephasing, and is then applied to find the distribution function and intervalence absorption cross section. To this end, the valence band is looked upon as an ensemble of two-level micro-ensembles, which are immersed in the homogeneous laser electric field. Within a single micro-ensemble the hole is treated quantum-mechanically with the help of modified Bloch equations, which, apart from Rabi oscillations and dephasing, also take into account particle feeding to and decay from the micro-ensemble (Breiland *et al* 1976). The transitions of the hole between different micro-ensembles are treated classically as in the standard MC method.

In this paper, the single-particle MC model is discussed and applied to calculation of the infrared (IR) absorption at low radiation intensities. The calculation of absorption in p-Ge at high CO_2 and NH_3 laser intensities, and comparison with the available experimental results, is presented in the second paper (Dargys 1989b).

2. Hole tunnelling dynamics in an intense laser field

In the following the spin–orbit split-off valence sub-band is neglected completely, and the remaining doubly degenerate heavy- and light-mass valence sub-bands are assumed to have spherical constant energy surfaces. Thus, the results obtained in this paper will be valid for laser energies $\hbar\omega$ smaller than the spin–orbit separation.

The laser field couples h and l sub-band wavefunctions. The invariance of the valence band effective-mass Hamiltonian to reflections with respect to the plane made up of hole wavevector and electric field allows one to construct linear wavefunction combinations, which remain decoupled even in the presence of the laser field (Aleshkin and Romanov 1984). These combinations, named positive and negative states, describe the dependence of the valence sub-band occupation on time, laser electric field amplitude and frequency, and initial wavevector. Specifically, the probability to find the hole in the l sub-band, p_l, when at the moment $t = 0$ the hole with certainty has been in the h sub-band and possessed wavevector $\boldsymbol{k}_0$, is (Dargys 1987)

$$p_l = \frac{\Omega^2 \sin^2[\frac{1}{2}\tau(\Omega^2 + \Delta^2)^{1/2}]}{\Omega^2 + \Delta^2}. \tag{1}$$

Here $\tau = \omega t$ is a dimensionless time, ω is the cyclic laser frequency, Ω is normalised to ω one-photon cyclic Rabi frequency

$$\Omega = (\sqrt{3}/2)\Theta\sqrt{n^2} \sin\theta \tag{2}$$

which depends on the angle θ (see figure 1) between initial hole wavevector $\boldsymbol{k}_0$ and

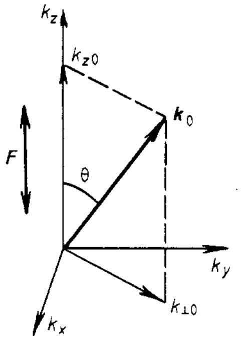

Figure 1. Orientation of laser electric field $\boldsymbol{F}$ and initial hole wavevector $\boldsymbol{k}_0$ with respect to coordinate axis.

harmonically varying electric field $\boldsymbol{F} = \boldsymbol{F}_0 \cos \omega t$, state index $n = \pm 1$ and dimensionless tunnelling constant

$$\Theta = \left(\frac{2\gamma\hbar^2}{m_0}\right)^{1/2} \frac{eF_0}{(\hbar\omega_r)^{3/2}}. \tag{3}$$

Here $\hbar\omega_r$ is the resonance energy, which is equal to the energy difference between light- and heavy-mass band energies at wavevector $\boldsymbol{k}_0$:

$$\hbar\omega_r = \varepsilon_l(\boldsymbol{k}_0) - \varepsilon_h(\boldsymbol{k}_0) = \hbar^2 2\gamma k_0^2/m_0$$

$4\gamma = m_h^{-1} - m_l^{-1}$ and e, m_0, $\hbar$ are elementary charge, free-electron mass and Planck's constant, respectively.

For us it is important that at not too large field amplitudes, more exactly when $\Theta \ll 1$, the Rabi frequencies for positive $n = +1$ and negative $n = -1$ states coincide. This property greatly simplifies the MC program because the doubly degenerate valence sub-bands can be viewed as if they are non-degenerate and, therefore, treated as a collection of simple two-level systems. However, it should be remembered that, at high laser intensities, when $\Theta \sim 1$, tunnelling between two degenerate valence sub-bands occurs with two different Rabi frequencies. For two-photon as well as for higher-order photon absorption, the Rabi frequencies, even at low intensities, are different for positive and negative states (Dargys 1987). In summary, the tunnelling probability (1) for spherical valence sub-bands depends on the relative detuning $\Delta = (\omega_r - \omega)/\omega$ and normalised Rabi frequency Ω in exactly the same manner as for a simple two-level system immersed in a harmonically varying electric field (Allen and Eberly 1975). This similarity allows us to consider the hole having initial wavevector $\boldsymbol{k}_0$ as an atomic two-level system. This is not evident at first sight, because in the field $\boldsymbol{F}_0 \cos \omega t$ the hole wavevector is not constant; in fact, the wavevector component parallel to the electric field changes according to the law

$$k_z(t) = k_{z0} + (eF_0/\hbar\omega) \sin \omega t \tag{4}$$

while the perpendicular one is time-independent, $k_\perp(t) = k_{\perp 0}$. At high intensities the oscillatory part of (4) can be large. Nevertheless, as the above arguments show, the hole with initial wavevector $\boldsymbol{k}_0 = (k_{z0}, k_{\perp 0})$ under the action of the laser field behaves as a simple two-level system characterised by level separation $\hbar\omega_r = \varepsilon_l(\boldsymbol{k}_0) - \varepsilon_h(\boldsymbol{k}_0)$.

3. Model for Monte Carlo simulation

3.1. Basic model

Figure 2 illustrates the basic model for calculation of inter-valence absorption of IR radiation due to transitions of the hole between heavy- and light-mass sub-bands. It

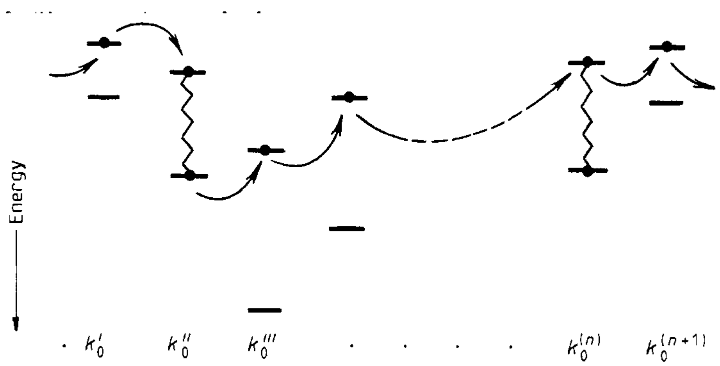

Figure 2. Two-level ensemble as a model for simulation of inter-valence absorption in p-type semiconductors. Owing to collisions with the phonons the hole hops among two-level systems characterised by different initial wavevectors $\boldsymbol{k}_0', \ldots, \boldsymbol{k}_0^{(n+1)}$. If separation between levels is close to the laser energy (vertical wavy lines) the hole undergoes Rabi oscillations, otherwise the hole before experiencing the next collision remains in pure upper or lower level characterised by energy $\varepsilon_h(\boldsymbol{k}_0'')$ and $\varepsilon_l(\boldsymbol{k}_0'')$.

consists of an ensemble of two-level systems, with the upper and lower level representing h and l sub-bands, respectively.

The different systems are labelled by hole wavevector components parallel, $k_{z0} = k_0 \cos\theta$, and perpendicular, $k_{\perp 0} = k_0 \sin\theta$, to the electric field, where θ is the angle between $\boldsymbol{k}_0$ and $\boldsymbol{F}_0$. An individual two-level system, in fact, is a micro-ensemble that consists of those holes which have equal $k_{\perp 0} = (k_{x0}^2 + k_{y0}^2)^{1/2}$ and k_{z0}. The hole can be scattered from one two-level system to another by lattice vibrations. For large detunings Δ, when the tunnelling probability is very small, the hole in the intervals between collisions stays on a single upper or lower level; its residence time on the level is equal to the free flight time in the respective sub-band. If the resonance condition is satisfied, the hole oscillates between upper and lower levels with the Rabi frequency. Now its residence time on the two-level system depends on the combination of free flight times in h and l sub-bands. This will be discussed in more detail in § 5.

3.2. Generalisation of the model

To describe the evolution of the simple two-level system, which is in contact with the reservoir (or other two-level systems) and at the same time is driven by an external force, the so-called Bloch equations are used (Blum 1981). However, these equations cannot be directly applied to our model in figure 2. The reason is that in the standard Bloch equations there is no exchange of particles between the considered two-level system and the reservoir, and as a result the particle stays on the two-level system forever.

In our model the particle number on the particular two-level system should be conserved only during the particle free flight time. To describe this situation we shall employ an open two-level model proposed by Breiland *et al* (1976), where particles can come into and leave the two-level system (figure 3). The open two-level system is described by the following four differential equations written in rotating-wave approximation (Breiland *et al* 1976)

$$\frac{\mathrm{d}p_r}{\mathrm{d}\tau} = -\Delta p_i - \frac{p_r}{\tau_2} \tag{5a}$$

$$\frac{\mathrm{d}p_i}{\mathrm{d}\tau} = \Delta p_r - \frac{p_i}{\tau_2} - \Omega(r_l - r_h) \tag{5b}$$

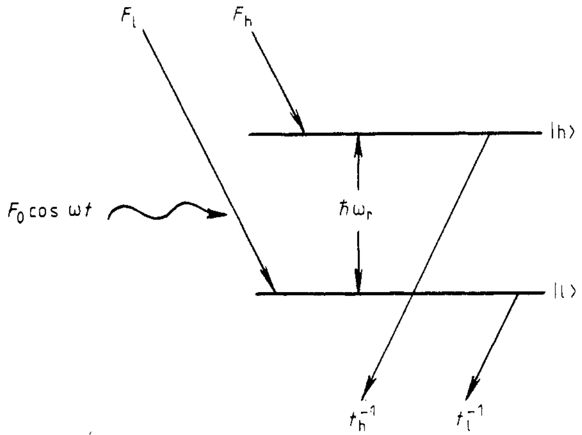

Figure 3. Pictorial description of an open two-level system. F_h and F_l are particle feeding rates and t_h^{-1} and t_l^{-1} are particle decay rates connected with heavy- and light-mass valence sub-bands.

$$\frac{dr_l}{d\tau} = \tfrac{1}{2}\Omega p_i - \frac{r_l}{\tau_l} + f_l \tag{5c}$$

$$\frac{dr_h}{d\tau} = -\tfrac{1}{2}\Omega p_i - \frac{r_h}{\tau_h} + f_h. \tag{5d}$$

In (5) r_l and r_h are probabilities to occupy the states $|l\rangle$ and $|h\rangle$ of the two-level system, respectively, and p_r and p_i are components that contain coherence information. These terms are connected to density matrix elements through relations

$$\rho_{11} = r_l \qquad \rho_{22} = r_h \qquad \rho_{21} = (p_r - ip_i)/2 \qquad \rho_{12} = (p_r + ip_i)/2.$$

$\tau_h = \omega t_h$ and $\tau_l = \omega t_l$ are dimensionless free flight times in decoupled h and l sub-bands,

$$\tau_2 = \omega t_2 = \left[\frac{1}{2}\left(\frac{1}{\tau_h} + \frac{1}{\tau_l}\right) + \frac{1}{\tau_2^*}\right]^{-1} \tag{6}$$

is a dimensionless dephasing (coherence) time, and $\tau_2^* = \omega t_2^*$ is a dimensionless pure dephasing time connected with extra mechanisms that spoil the coherence of individual dipoles in the micro-ensemble. Equation (6) is an exact analogue of the transverse relaxation time in the standard Bloch equations. $f_l = F_l/\omega$ and $f_h = F_h/\omega$ are dimensionless feeding rates, which do not depend explicitly on the laser intensity. The feeding is assumed to occur to the pure $|l\rangle$ and $|h\rangle$ states, not to their superposition. In the absence of the driving field, $\Omega = 0$, (5*a*) and (5*b*) are decoupled from the rest of the equations, and their solution describes the exponential decay of the permanent dipole. In (5) the term responsible for relaxation from $|l\rangle$ to $|h\rangle$ states, which is so important in the standard Bloch system, is omitted, because in semiconductors direct transitions between valence sub-bands, wherein the hole due to collision with the phonon performs an inter-valence transition without momentum change, is forbidden by momentum conservation.

The system (5), in general, does not conserve the probability to find the particle on the considered two-level system during hole free flight time. The MC method, although governed by probabilistic laws, is classical in nature. This means that between the collisions the joint probability to find the particle in $|h\rangle$ and $|l\rangle$ states should be independent of time and satisfy $r_h(t) + r_l(t) = 1$, and that after the collision the whole particle, not part of it, should be transferred to the other two-level system, otherwise there will be particle probability leakage. The particle conservation equation, $r_h(t) + r_l(t) = 1$, along with (5*c*) and (5*d*) yields the balance equation between the feeding and decay:

$$f_l + f_h = r_l/\tau_l + r_h/\tau_h = \tau_h^{-1} + (\tau_l^{-1} - \tau_h^{-1})r_l.$$

To advance further, something about feeding terms should be assumed. In the following the feeding term of the light-hole-mass sub-band will be equated to the equilibrium value $f_l \simeq f_l^{(0)} = r_l^{(0)}/\tau_l$. Such approximation is expected to be good for large laser energies when in the region of excitation $r_l^{(0)} \simeq 0$. With this in mind, the system (5) reduces to

$$\frac{\mathrm{d}p_r}{\mathrm{d}\tau} = -\Delta p_i - \frac{p_r}{\tau_2} \tag{7a}$$

$$\frac{\mathrm{d}p_i}{\mathrm{d}\tau} = \Delta p_r - \frac{p_i}{\tau_2} - \Omega(2r_l - 1) \tag{7b}$$

$$\frac{\mathrm{d}r_l}{\mathrm{d}\tau} = \tfrac{1}{2}\Omega p_i - \frac{r_l - r_l^{(0)}}{\tau_l} \tag{7c}$$

which bears a very close resemblance to the standard Bloch equations (Allen and Eberly 1975, Blum 1981). However, there is a fundamental difference: in the system (7) the change of population on $|\mathrm{h}\rangle$ and $|\mathrm{l}\rangle$ levels occurs through other two-level systems, while in the standard Bloch equations the population relaxes within a single two-level system, although in both cases $r_h(t) + r_l(t) = 1$.

Two types of solutions of (7), stationary (s) and transient (t), were incorporated into the MC program. Of all possible solutions they, in some sense, are 'extreme', and in the following will be referred to as s-case and t-case, respectively.

The *s-case* assumes that between collisions the two-level evolution can be approximated by stationary solutions of (7). Equating all derivatives to zero, the following expressions for the imaginary part of the component which contains coherence information and $|\mathrm{l}\rangle$-state population are found:

$$p_{is} = \frac{\Omega\tau_2(1 - 2r_l^{(0)})}{1 + \Omega^2\tau_2\tau_l + \Delta^2\tau_2^2)} \tag{8}$$

$$r_{ls} = \frac{\tfrac{1}{2}\Omega^2\tau_2\tau_l + r_l^{(0)}(1 + \Delta^2\tau_2^2)}{1 + \Omega^2\tau_2\tau_l + \Delta^2\tau_2^2}. \tag{9}$$

In the limit of very intense fields, when $\Omega \to \infty$, (9) reduces to $r_{ls} = \frac{1}{2}$, which means that in this limit the population difference $r_{hs} - r_{ls}$ is zero.

The *t-case* assumes that after the scattering the hole evolution can be described by a transient solution of (7) with the initial conditions $p_i(\tau = 0) = 0$, $p_r(\tau = 0) = 0$ and $r_l(\tau = 0) = r_l^{(0)} \simeq 0$, if at $\tau = 0$ the hole was scattered into the h sub-band, or $r_l(\tau = 0) = 1 - r_l^{(0)} \simeq 1$, if at $\tau = 0$ it was scattered into the l sub-band. The transient solution of (7) under various initial conditions has been discussed by Torrey (1949). In the particular case when $\tau_2, \tau_l \to \infty$ and $p_i(0) = p_r(0) = r_l(0) = 0$ one can easily find that

$$p_i = \frac{-\Omega}{(\Omega^2 + \Delta^2)^{1/2}} \sin[\tau(\Omega^2 + \Delta^2)]^{1/2} \tag{10}$$

$$r_l = \frac{\Omega^2 \sin^2[\tfrac{1}{2}\tau(\Omega^2 + \Delta^2)^{1/2}]}{\Omega^2 + \Delta^2}. \tag{11a}$$

If the hole at $\tau = 0$ has been scattered into the l sub-band, $r_l(0) = 1$, $p_i(0) = p_r(0) = 0$, equation (11a) should be replaced by

$$r_l' = 1 - r_l. \tag{11b}$$

The probability (11a) to find the hole at the moment τ in the l sub-band, coincides with the expression (1) for tunnelling probability. Of course, in (1) and (11a) the concrete expression for the normalised Rabi frequency Ω can be found only from the Schrödinger equation for degenerate valence bands (Dargys 1987).

4. Absorption cross section

Below, the relations between p_i and absorption cross section due to hole transitions between l and h sub-bands are discussed. More general considerations can be found in Allen and Eberly (1975).

First, it will be assumed that the electric field amplitude is a slowly varying function of coordinate z: $\partial F_0/\partial z \ll 2\pi F_0/\lambda_s$. This means that over the laser wavelength λ_s in the semiconductor the change of F_0 is small. Secondly, the amplitude F_0 is assumed to be time-independent, because in the ensemble of two-level systems having different $\hbar\omega_r$ we do not expect radiation trapping effects, such as the breakdown of radiation pulse inside the crystal into 2π pulses (McCall and Hahn 1969). Then, the wave equation for linearly polarised light and two-level equations (7) yield the following relation between light intensity I and p_i:

$$\frac{\mathrm{d}I}{\mathrm{d}z} = N\left\langle\frac{\hbar\omega}{2}\bar{\Omega}p_i\right\rangle \tag{12a}$$

where N is hole concentration and $\bar{\Omega} = \Omega\omega$ is Rabi frequency related to the average dipole moment d through the relation $\bar{\Omega} = dF_0/\hbar$. Brackets $\langle\ldots\rangle$ mean an average over the two-level ensemble, which in the case of the MC method is done automatically during simulation. Equation (12a) can be rewritten the form of a non-linear Bouguer–Lambert–Beer law (Allen and Eberly 1975)

$$\mathrm{d}I/\mathrm{d}z = N\langle\sigma\rangle I \tag{12b}$$

$$\langle\sigma\rangle = \frac{\hbar\omega}{2I}\langle\bar{\Omega}p_i\rangle \tag{13}$$

where $\langle\sigma\rangle$ is the total absorption cross section, which now depends on the scattering rate with phonons and on the light intensity

$$I = \frac{F_0^2\varepsilon_0\varepsilon}{2}\frac{c}{n}. \tag{14}$$

In (14), c is the light velocity, ε_0 is the permittivity of the vacuum, ε is the relative dielectric constant of the semiconductor and $n \simeq \sqrt{\varepsilon}$ is the index of refraction. It should be noted that in (14) the amplitude of the electric field F_0 is measured inside the semiconductor, and I corresponds to the total intensity, including lattice polarisation. In a special case, when the semiconductor surface is covered with an anti-reflection coating, I equals the light intensity in vacuum and F_0 equals the electric field amplitude inside the semiconductor at the vacuum–semiconductor interface.

It is convenient to divide the total cross section (13) into two parts, the cross section associated with pure absorption $\langle\sigma\rangle_a$ and that associated with induced emission $\langle\sigma\rangle_e$:

$$\langle\sigma\rangle = \langle\sigma\rangle_a - \langle\sigma\rangle_e. \tag{15}$$

In the s-case, $\langle\sigma\rangle_a$ and $\langle\sigma\rangle_e$ include all simulation events (and corresponding p_i values), wherein the scattered hole is transferred to h sub-band and l sub-band, respectively. In the t-case, $\langle\sigma\rangle_a$ and $\langle\sigma\rangle_e$ correspond to those events where hole inter-sub-band transitions h $\rightarrow$ l and l $\rightarrow$ h take place.

Equation (13) can be used directly in the MC program if p_i is equal to its stationary value (8). In the t-case, when (10) and (11) are used, p_i has been replaced by a value averaged over the free flight time, $t_{FF} = \tau_{FF}/\omega$

$$\bar{p}_i = \frac{1}{\tau_{FF}} \int_0^{\tau_{FF}} p_i(\tau)\,d\tau = -\frac{2}{\tau_{FF}\Omega} \begin{cases} r_l(\tau_{FF}) & \text{if tunnelling begins from h sub-band} \\ r_l(\tau_{FF}) - 1 & \text{if tunnelling begins from l sub-band.} \end{cases} \tag{16}$$

In (16) $\tau = 0$ corresponds to the moment just after the scattering event. Then, from (13), (14) and (16) it follows that

$$I\langle\sigma\rangle_a = -\langle \hbar\omega r_l(t_{FF})/t_{FF}\rangle \tag{17a}$$

$$I\langle\sigma\rangle_e = \langle \hbar\omega[1 - r_l(t_{FF})]/t_{FF}\rangle. \tag{17b}$$

These expressions can be interpreted as an average energy absorbed and emitted by a hole over its free flight time, or equivalently as the power absorbed and emitted by a single hole.

5. Flight duration

An intense laser field mixes valence sub-bands, especially in the resonance region. Since decoupled sub-band free flight times $t_h(\boldsymbol{k}_0)$ and $t_l(\boldsymbol{k}_0)$ are not equal, frequently $t_l(\boldsymbol{k}_0) \ll t_h(\boldsymbol{k}_0)$, the hole free flight time in the mixed bands will depend on laser intensity.

5.1. *The s-case*

If the probabilities r_l and r_h to find the hole in l and h sub-bands are time-independent, the combined probability that a hole in the state $\boldsymbol{k}_0$ suffers a collision during the time interval dt will be $r_l dt/t_l + r_h dt/t_h$. Then, reasoning exactly along the same lines as in a single-sub-band case (Jacoboni and Reggiani 1983) yields the following formula for the average free flight time t_{FF} in laser-coupled sub-bands:

$$\frac{1}{t_{FF}} = \frac{r_l}{t_l} + \frac{r_h}{t_h} = \frac{1}{t_h} + \left(\frac{1}{t_l} - \frac{1}{t_h}\right) r_l. \tag{18}$$

The free flight duration was generated with the aid of the formula $t_r = -t_{FF} \ln r$, where r is a random number between 0 and 1.

5.2. *The t-case*

The transient case is more complicated. Here it is useful to remind ourselves that in a single-band case the probability to find the flight duration t_r, if an average free flight time is t_{FF}, is given by $P_{FF} = t_{FF}^{-1} \exp(-t_r/t_{FF})$. This can be interpreted as a probability of disintegration of a one-level particle, whose average lifetime on the level is t_{FF}. If one has a two-level particle (system) with disintegration times t_h and t_l on the respective levels, then due to wavefunction mixing the resulting lifetime of the two-level particle immersed in an alternating electric field is the average of t_h and t_l, and acquires an additional beat factor. The lifetime can be found from the following pair of differential equations (Rautian *et al* 1979):

$$\frac{da_h}{d\tau} = -\frac{a_h}{2\tau_h} + \frac{\Omega}{2} e^{-i\Delta\tau} a_l \tag{19a}$$

$$\frac{da_l}{d\tau} = -\frac{a_l}{2\tau_l} - \frac{\Omega}{2} e^{i\Delta\tau} a_h. \tag{19b}$$

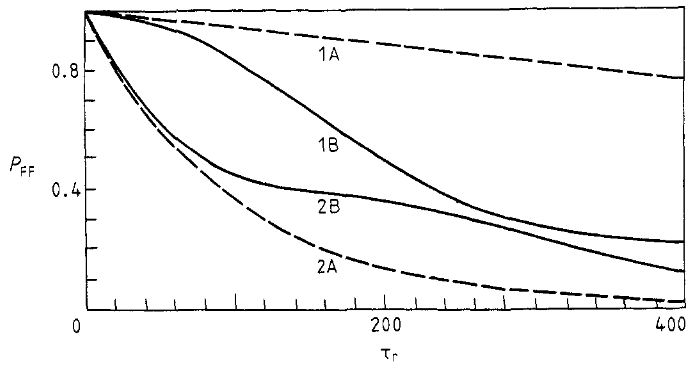

Figure 4. The probability distribution that the hole has not suffered a collision with phonons during its free flight $\tau_r = \omega t_r$ (ω is cyclic frequency of the IR laser), when the laser is switched off (curves 1A, 2A) and when the laser is switched on (curves 1B, 2B). For curves 1A and 1B the hole at the moment $\tau = 0$ was in h sub-band, and for curves 2A and 2B it was in l sub-band. $\tau_h = 1500$, $\tau_l = 100$, $\Omega = 0.0149$, $\Delta = 0.007$.

Then, the probability that at the moment $\tau_r = \omega t_r$ the particle has not disintegrated (or in terminology of holes, the probability that in a mixed state the hole has not experienced the collision) is given by

$$P_{FF} = a_h a_h^* + a_l a_l^*. \tag{20}$$

The initial conditions for 'wavefunctions' a_h and a_l are the following. If at $t = 0$ after the last collision the hole is in the h sub-band, then $a_h = 1$, $a_l = 0$, and if the hole is in the l sub-band, then $a_h = 0$, $a_l = 1$.

Some characteristic solutions of (19) are summarised below. For zero electric field ($\Omega = 0$) the equations are decoupled, and their solutions are $P_{FF} = \exp(-\tau_r/\tau_l)$ or $P_{FF} = \exp(-\tau_r/\tau_h)$. They describe the probability to find the free flight time τ_r of the hole in h and l sub-bands, respectively (curves 1A and 2A in figure 4). If $\tau_h = \tau_l$, then P_{FF} is independent of electric field and detuning Δ, and equals $P_{FF} = \exp(-\tau_r/\tau_l)$. In the case of infinite lifetimes (τ_h, $\tau_l \to \infty$) the probability $P_{FF} = 1$, and $|l\rangle$-state population $a_l a_l^*$ changes according to (1) and (11*a*). Since the general solution of (19) is a rather complicated expression (it can be found in Rautian *et al* (1979)) here only some typical curves will be presented. Figure 4 illustrates the unnormalised probability density for a hole flight duration in p-Ge at 77 K and under CO_2 laser irradiation ($F_0 = 10\ \mathrm{kV\ cm^{-1}}$). As seen, in the presence of IR irradiation the probability P_{FF} oscillates with frequency $\omega\Omega/2$ due to hole tunnelling between sub-bands and satisfies $\exp(-\tau/\tau_l) < P_{FF}(\tau) < \exp(-\tau/\tau_h)$.

In the MC program the flight duration was generated with the help of formulae $t_r = -t_{FF} \ln r$ and (18) in the s-case, or with the Neumann rejection technique (Jacoboni and Reggiani 1983) in the t-case. In the latter case a pair of random numbers was cast along the ordinate and abscissa axis and only those points which fell below the curves $P_{FF}(\tau_r)$ of the type in figure 4 were accepted.

In constructing various histograms one needs to know the residence time, i.e. time the hole has stayed in the particular level during its free flight. The residence time in the $|l\rangle$ level was calculated with the formula

$$t_{Fl} = \int_0^{t_{FF}} r_l(t)\, \mathrm{d}t. \tag{21}$$

Since $r_l(t) + r_h(t) = 1$, the residence time in $|h\rangle$ level is

$$t_{\mathrm{Fh}} = \int_0^{t_{\mathrm{FF}}} r_{\mathrm{h}}(t)\,\mathrm{d}t = t_{\mathrm{FF}} - t_{\mathrm{Fl}}. \tag{22}$$

For the s-case r_{l} is time-independent. Then, $t_{\mathrm{Fl}} = r_{\mathrm{l}} t_{\mathrm{FF}}$ and $t_{\mathrm{Fh}} = r_{\mathrm{h}} t_{\mathrm{FF}}$. These expressions have very clear physical meaning.

For the t-case, after insertion of (11a) into (21), one finds

$$t_{\mathrm{Fl}} = \frac{t_{\mathrm{FF}}\Omega}{2(\Omega^2+\Delta^2)}\left(1 - \frac{\sin[\tau_{\mathrm{FF}}(\Omega^2+\Delta^2)^{1/2}]}{\tau_{\mathrm{FF}}(\Omega^2+\Delta^2)^{1/2}}\right). \tag{23}$$

6. Monte Carlo averages

The average of physical quantity q in h and l sub-bands is expressed through the distribution functions $f_{\mathrm{h}}(\boldsymbol{k})$ and $f_{\mathrm{l}}(\boldsymbol{k})$:

$$\langle q_{\mathrm{h,l}}\rangle = \int f_{\mathrm{h,l}}(\boldsymbol{k}) q_{h,l}(\boldsymbol{k})\,\mathrm{d}\boldsymbol{k} \Big/ \int f(\boldsymbol{k})\,\mathrm{d}\boldsymbol{k} \tag{24}$$

where $f(\boldsymbol{k}) = f_{\mathrm{h}}(\boldsymbol{k}) + f_{\mathrm{l}}(\boldsymbol{k})$. The role of the distribution function, which describes the probability to detect the particle in a small volume element in $\boldsymbol{k}$-space, is played by the time the particle has visited the considered volume element during MC simulation. With this in mind, for example, the average MC absorption and emission cross sections can be written as

$$\langle\sigma\rangle_{\mathrm{a}} = \sum_{\mathrm{coll}} \tau_{\mathrm{Fh}}\sigma_{\mathrm{a}} \Big/ \sum_{\mathrm{coll}} \tau_{\mathrm{FF}} \tag{25}$$

$$\langle\sigma\rangle_{\mathrm{e}} = \sum_{\mathrm{coll}} \tau_{\mathrm{Fl}}\sigma_{\mathrm{e}} \Big/ \sum_{\mathrm{coll}} \tau_{\mathrm{FF}} \tag{26}$$

where summation is over all possible collisions (equivalently, over all two-level systems the hole has visited), and σ_{a}, σ_{e} are elementary absorption and emission cross sections $\sigma_{\mathrm{a,e}} = (\hbar\omega/2I)\bar{\Omega} p_{\mathrm{ia,e}}$ (cf. (13) and (15)).

Similarly, the average hole energy in the nth cell of the h sub-band is

$$\langle\varepsilon_{\mathrm{h}}(n)\rangle = \sum_{\mathrm{coll}\,n} \tau_{\mathrm{Fh}}\varepsilon_{\mathrm{h}}(n) \Big/ \sum_{\mathrm{coll}} \tau_{\mathrm{FF}} \tag{27}$$

where coll n indicates that in the summation only those collisions which have occurred in the nth cell of $(k_z, k_\perp)$-space are included. To find the average energy in the h sub-band one has to sum over all cells

$$\langle\varepsilon_{\mathrm{h}}\rangle = \sum_n \langle\varepsilon_{\mathrm{h}}(n)\rangle. \tag{28}$$

7. Block diagram of the Monte Carlo program

Figure 5 summarises the main steps of the MC procedure for calculation of inter-valence absorption. The following comments are appropriate.

(1) After the data input, the initial values (sub-band index b = h, l, wavevector $\boldsymbol{k}_0 = (k_{z0}, k_{\perp 0})$) are assigned to the hole.

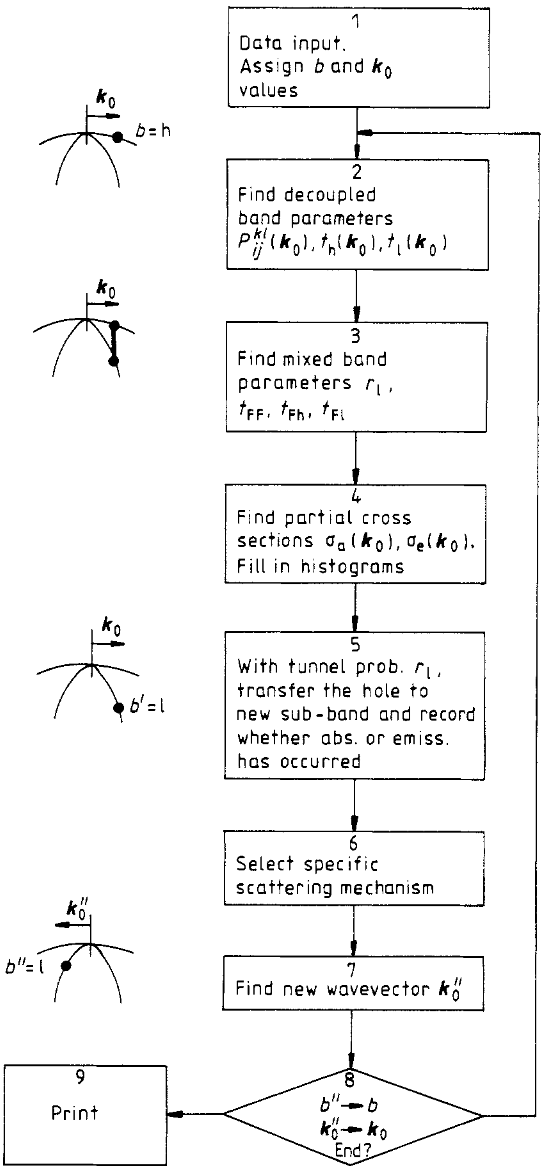

Figure 5. Flowchart of the Monte Carlo program.

(2) The decoupled sub-band hole scattering probabilities $P_{ij}^{kl}(\boldsymbol{k}_0)$ per unit time are calculated. Inter-sub-band ($ij = \mathrm{hl}$ or $ij = \mathrm{lh}$) and intra-sub-band ($ij = \mathrm{hh}$ or $ij = \mathrm{ll}$) scattering with acoustic and optic ($k = \mathrm{a}$ or $k = \mathrm{o}$) phonon absorption and emission ($l = \mathrm{a}$ or $l = \mathrm{e}$) are taken into account—all in all 16 scattering mechanisms (for details see Appendix).

With known $P_{ij}^{kl}(\boldsymbol{k}_0)$ the free flight times in decoupled sub-bands are determined:

$$t_\mathrm{h}(\boldsymbol{k}_0) = [P_{\mathrm{hh}}^{\mathrm{aa}} + P_{\mathrm{hh}}^{\mathrm{ae}} + P_{\mathrm{hl}}^{\mathrm{aa}} + P_{\mathrm{hl}}^{\mathrm{ae}} + P_{\mathrm{hh}}^{\mathrm{oa}} + P_{\mathrm{hh}}^{\mathrm{oe}} + P_{\mathrm{hl}}^{\mathrm{oa}} + P_{\mathrm{hl}}^{\mathrm{oe}}]^{-1} \tag{29}$$

$$t_\mathrm{l}(\boldsymbol{k}_0) = [P_{\mathrm{ll}}^{\mathrm{aa}} + P_{\mathrm{ll}}^{\mathrm{ae}} + P_{\mathrm{lh}}^{\mathrm{aa}} + P_{\mathrm{lh}}^{\mathrm{ae}} + P_{\mathrm{ll}}^{\mathrm{oa}} + P_{\mathrm{ll}}^{\mathrm{oe}} + P_{\mathrm{lh}}^{\mathrm{oa}} + P_{\mathrm{lh}}^{\mathrm{oe}}]^{-1}. \tag{30}$$

(3) Using $t_\mathrm{h}(\boldsymbol{k}_0)$ and $t_\mathrm{l}(\boldsymbol{k}_0)$, the parameters characteristic of sub-bands coupled by a laser field are calculated:

(i) coupled-sub-band hole free flight time $t_{\mathrm{FF}}(\boldsymbol{k}_0)$;

Table 1. Constants of p-Ge used in MC program.

Quantity	Symbol	Value	Unit
Sound velocity	u	5.4×10^5	$\mathrm{cm\ s^{-1}}$
Density	ρ	5.32	$\mathrm{g\ cm^{-3}}$
Optic deformation potential	$D_t K$	9×10^8	$\mathrm{eV\ cm^{-1}}$
Optic phonon energy	$\varepsilon_{\mathrm{op}}$	37.4	meV
Heavy mass	m_{h}	0.34	
Light mass	m_{l}	0.05	
Acoustic phonon scattering rate[a]	$a\varepsilon^b$	—	$\mathrm{s^{-1}}$

[a] Values of the constants a and b for phonon absorption and emission by light and heavy holes of energy ε are presented in Appendix 2 of paper II.

(ii) h and l sub-band populations at wavevector $\boldsymbol{k}_0$ and at moment t_{FF};

(iii) residence times in coupled h and l sub-bands $t_{\mathrm{Fh}}(\boldsymbol{k}_0)$ and $t_{\mathrm{Fl}}(\boldsymbol{k}_0)$ for construction of distribution functions and averages.

(4) Partial absorption $\sigma_{\mathrm{a}}(\boldsymbol{k}_0)$ and emission $\sigma_{\mathrm{e}}(\boldsymbol{k}_0)$ cross sections are found. Using $t_{\mathrm{Fh}}(\boldsymbol{k}_0)$ and $t_{\mathrm{Fl}}(\boldsymbol{k}_0)$ as weights, the values of various physical parameters which correspond to wavevector $\boldsymbol{k}_0$ are summed up into appropriate cells for construction of histograms and various averages.

(5) Using $r_{\mathrm{l}}(\boldsymbol{k}_0)$ as the probability for a hole to suffer tunnelling transitions h $\rightarrow$ l (if initially the hole was in h sub-band) or l $\rightarrow$ h (if initially the hole was in l sub-band), the hole is transferred into appropriate sub-band b'. If tunnelling transition h $\rightarrow$ l (l $\rightarrow$ h) has occurred the absorption (emission) of radiation quanta $\hbar\omega$ is recorded. If tunnelling transition has not occurred, it is assumed that no interaction of radiation with the hole has taken place.

(6) Specific scattering mechanism and the sub-band b'' into which the hole is to be scattered by the phonon are selected. For this purpose the probabilities $P_{ij}^{kl}(\boldsymbol{k}_0)$ found in step 2 as well as information to which sub-band the hole has tunnelled (for example, into $b = \mathrm{l}$, see step 5) are used.

(7) New hole wavevector $\boldsymbol{k}_0''$ is calculated.

(8) The initial hole wavevector and sub-band index are renamed ($\boldsymbol{k}_0'' \rightarrow \boldsymbol{k}_0$, $b'' \rightarrow b$), and the MC procedure is continued beginning from step 2. If the total number of scattering events with phonons is sufficient the MC simulation is interrupted and results, histograms, etc., are printed.

8. Low-intensity absorption

All MC calculations in this (and the next) paper were done with $r_{\mathrm{l}}^{(0)} = 0$. The constants used in the MC program are presented in table 1.

In figure 6 the inter-valence absorption and induced emission cross sections defined by (25) and (26) are plotted as a function of laser energy $\hbar\omega$ at weak laser intensities. The experimentally accessible cross section is the difference $\langle\sigma\rangle = \langle\sigma\rangle_{\mathrm{a}} - \langle\sigma\rangle_{\mathrm{e}}$. In the program inter-valence tunnelling was taken into account if detuning appeared to be in the range $-0.25 \leqslant \Delta \leqslant 0.25$. For larger and smaller Δ values the simulation proceeded as if radiation was switched off and sub-bands decoupled altogether. Everywhere in obtaining a single point about 10^5 collisions with phonons have been simulated. The full curves in figure 6 are analytical expressions

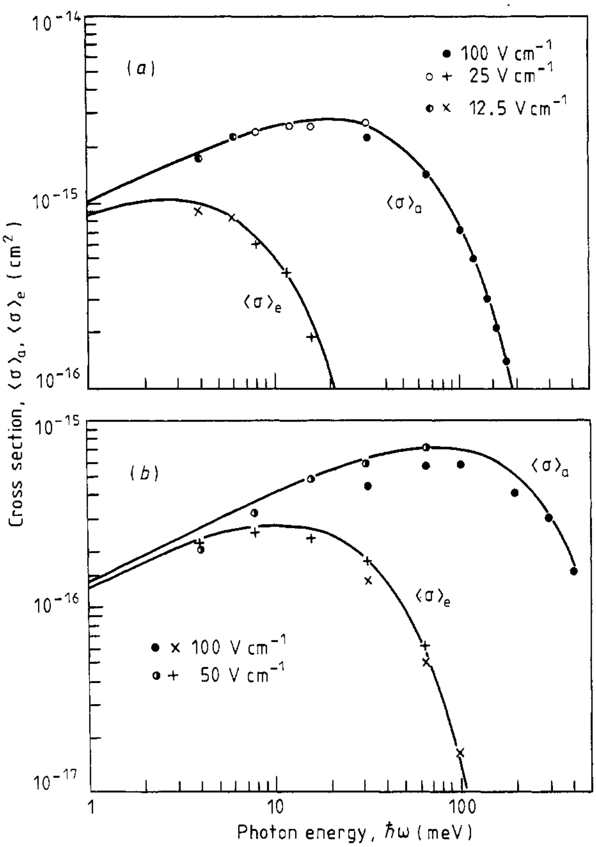

Figure 6. Dependence of the absorption $\langle\sigma\rangle_a$ and induced emission $\langle\sigma\rangle_e$ cross sections on the laser energy in the limit of low intensities: (*a*) s-case, $T = 77$ K; (*b*) t-case, $T = 300$ K. Points are Monte Carlo calculations and curves are analytical results.

$$\langle\sigma\rangle_a = \frac{2\pi^{3/2}}{\sqrt{\varepsilon}} \frac{\alpha}{(m_h/m_0)[1+(m_l/m_h)^{3/2}]} \frac{1}{(m_h/m_l - 1)^{1/2}} \frac{\hbar^2(\hbar\omega)^{1/2}}{m_0(kT)^{3/2}} \times \exp\left(-\frac{\hbar\omega}{kT}\frac{1}{m_h/m_l - 1}\right) \tag{31}$$

$$\langle\sigma\rangle_e = \frac{2\pi^{3/2}}{\sqrt{\varepsilon}} \frac{\alpha}{(m_l/m_0)[1+(m_h/m_l)^{3/2}]} \frac{1}{(1 - m_l/m_h)^{1/2}} \frac{\hbar^2(\hbar\omega)^{1/2}}{m_0(kT)^{3/2}} \times \exp\left(-\frac{\hbar\omega}{kT}\frac{1}{1 - m_l/m_h}\right) \tag{32}$$

which can be deduced with the equilibrium distribution functions in h and l sub-bands, inter-valence band transition matrix elements calculated within first-order perturbation theory, and energy-conserving δ-function. In (31) and (32) α is fine structure

$$\alpha = e^2/(4\pi\varepsilon_0\hbar c) \simeq 137.$$

Some remarks are to be pointed out in connection with figure 6. First of all, in calculating cross sections by the MC method here (and in all figures which will be presented in paper II) no adjustable parameters were used. Secondly, the cross sections calculated by the MC method are slightly smaller, especially in figure 6(*b*). This is connected with the finite electric field amplitude used in the MC simulation, and as a result the slight perturbation of the distribution function in the region of the resonance.

Low electric field intensities lead to very narrow absorption linewidths (compare (8)–(11a)) and many collisions are needed to get reliable results, especially at small $\hbar\omega$ values. Thirdly, in the cross sections, as already mentioned, the distribution function plays the role of flight duration in the respective sub-bands. The cross sections as seen from (25) and (26) explicitly depend on the scattering rates P_{ij}^{kl}. As known, low-intensity cross sections, in fact, are independent of scattering rates. That this is indeed the case has been checked by varying the acoustic phonon scattering rate: at low fields the MC cross sections (25) and (26) were found to be independent of P_{ij}^{kl}. This is so, because at low fields the MC procedure itself automatically ensures the detailed balance between in-scattering and out-scattering processes. For the same reason the low-field expressions (31) and (32) do not contain parameters which govern the scattering, for example, deformation potential constants. However, at high laser intensities, when detailed balance is not necessarily satisfied, the cross section does depend on phonon scattering rate, as will be seen in paper II. Finally, the reliability of the MC procedure has been checked with the equilibrium analytical solution with no adjustable parameters. At low field amplitudes both the transient case and the stationary case formulae yield good agreement with the analytical calculations and at this stage no preference can be given to either.

Appendix. Final state after scattering

Let $\boldsymbol{k}_{\rm i}$ and $\boldsymbol{k}_{\rm f}$ be initial hole wavevector before scattering and final wavevector after scattering, respectively, and Θ the angle between them. The polar $\theta_{\rm f}$ and azimuthal $\varphi_{\rm f}$ angles of $\boldsymbol{k}_{\rm f}$ were generated with two random numbers r_1 and r_2 distributed evenly between 0 and 1

$$\cos\theta_{\rm f} = 1 - 2r_1 \tag{A1}$$

$$\varphi_{\rm f} = 2\pi r_2. \tag{A2}$$

The angles were accepted if intra-sub-band, $G_{ii} = (1 + 3\cos^2\Theta)/4$, and inter-sub-band, $G_{ij} = 3(1 - \cos^2\Theta)/4$, overlap factors satisfied $G_{ii}, G_{ij} > r_3$, where r_3 is also a random number; otherwise new angles $\theta_{\rm f}$ and $\varphi_{\rm f}$ were generated with (A1) and (A2). The modulus of $\boldsymbol{k}_{\rm f}$ was found from momentum and energy conservation

$$\boldsymbol{k}_{\rm f} = \boldsymbol{k}_{\rm i} \pm \boldsymbol{q} \tag{A3}$$

$$\frac{\hbar^2 k_{\rm f}^2}{2m_{\rm f}} = \frac{\hbar^2 k_{\rm i}^2}{2m_{\rm i}} \pm \hbar q u \tag{A4}$$

in the case of acoustic phonon scattering, and from energy conservation only

$$\frac{\hbar^2 k_{\rm f}^2}{2m_{\rm f}} = \frac{\hbar^2 k_{\rm i}^2}{2m_{\rm i}} \pm \varepsilon_{\rm op} \tag{A5}$$

in the case of optical phonon scattering. Here $m_{\rm f}$ and $m_{\rm i}$ are final and initial hole masses ($m_{\rm f}$, $m_{\rm i} = m_{\rm h}$, $m_{\rm l}$) and u is the sound velocity. The upper (lower) sign corresponds to absorption (emission) of a phonon with energy $\hbar q u$ or $\varepsilon_{\rm op}$. Finally $\boldsymbol{q}$ is the acoustic phonon wavevector. The system (A3), (A4) was solved by a special fast iterative procedure. If selected random numbers r_1, r_2, r_3 did not allow (A3) and (A4) to be satisfied simultaneously, a new scattering mechanism was determined stochastically and a new final-state vector calculated.

References

Aleshkin V Ya and Romanov Yu A 1984 *Zh. Eksp. Teor. Fiz.* **87** 1857
Allen L and Eberly J H 1975 *Optical Resonance and Two-level Atoms* (New York: Wiley)
Blum K 1981 *Density Matrix Theory and Application* (New York: Plenum)
Breiland W G, Fayer M D and Harris C B 1976 *Phys. Rev.* A **13** 383
Dargys A 1987 *Phys. Status Solidi* b **143** 675
—— 1989a *Liet. Fiz. Rinkinys* **29** 298, 722
—— 1989b *J. Phys.: Condens. Matter* **1** 9653
Gibson A F 1972 *Appl. Phys. Lett.* **21** 356
Jacoboni C and Reggiani L 1983 *Rev. Mod. Phys.* **55** 645
James R B and Smith D L 1982 *IEEE J. Quantum Electron.* **18** 1841
McCall S L and Hahn E L 1969 *Phys. Rev.* **183** 457
Pearsall T P, Nahory R E and Chelikowski J R 1977 *Phys. Rev. Lett.* **39** 295
Rautian S G, Smirnov G I and Shalagin A M 1979 *Nonlinear Resonances in Atomic and Molecular Spectra* (in Russian) (Moscow: Nauka)
Torrey H C 1949 *Phys. Rev.* **76** 1059
Zener C 1934 *Proc. R. Soc.* A **145** 523